Transport control in a deterministic ratchet system

Woo-Sik Son,[1,*] Jung-Wan Ryu,[2] Dong-Uk Hwang,[3] Soo-Young Lee,[4] Young-Jai Park,[5,†] and Chil-Min Kim[1,‡]
[1]*National Creative Research Initiative Center for Quantum Chaos Applications, Sogang University, Seoul 121-742, Korea*
[2]*Department of Physics, Pusan National University, Busan 609-735, Korea*
[3]*Department of Biomedical Engineering, University of Florida, Gainesville, Florida 32611-6131, USA*
[4]*Department of Physics, Seoul National University, Seoul 151-747, Korea*
[5]*Department of Physics, Sogang University, Seoul 121-742, Korea*
(Received 16 December 2006; revised manuscript received 10 March 2008; published 19 June 2008)

We study the control of transport properties in a deterministic inertia ratchet system via the extended delay feedback method. A chaotic current of a deterministic inertia ratchet system is controlled to a regular current by stabilizing unstable periodic orbits embedded in a chaotic attractor of the unperturbed system. By selecting an unstable periodic orbit, which has a desired transport property, and stabilizing it via the extended delay feedback method, we can control transport properties of the deterministic inertia ratchet system. Also, we show that the extended delay feedback method can be utilized for separation of particles in the deterministic inertia ratchet system as a particle's initial condition varies.

DOI: 10.1103/PhysRevE.77.066213 PACS number(s): 05.45.Gg, 05.40.−a, 05.45.Pq, 05.60.Cd

I. INTRODUCTION

The ratchet effect, i.e., a directional motion of a particle using unbiased fluctuations, has attracted much attention in recent years [1,2]. An early motivation in this field is to explain an underlying mechanism of molecular motors which transport molecules in the absence of appropriate potential and thermal gradients [3]. The leading works in Refs. [4] and [5] open studies on the Hamiltonian ratchets [6] and the inertia ratchets [7], respectively. Later, the ratchet effect has been studied theoretically and experimentally in many different fields of science, e.g., asymmetric superconducting quantum interference devices [8], quantum Brownian motion [9], Josephson-junction arrays [10], application for separation of particles [11], quenched disordered systems [12], etc. It has been known that two conditions should be met to obtain the ratchet effect [1]. First, a system has to be in a nonequilibrium state by a correlated stochastic [13] or a deterministic perturbation [14]. Second, the breaking of the spatial inversion symmetry is required. In doing so, an asymmetric periodic potential, named the "ratchet potential," is introduced.

In particular, several works concerning the control of ratchet dynamics have been presented. The applying of a weak subharmonic driving in a deterministic inertia ratchet system was used to enlarge the parameter ranges where regular currents are observed [15], and the signal mixing of two driving forces was considered to control transport properties in an overdamped ratchet system [16]. Also, the effect of time-delayed feedback [17] has been studied in ratchet systems [18]. Moreover, the anticipated synchronization was observed in delay coupled inertia ratchet systems [19] and the stabilization of chaotic current to low-period orbits was presented, using time-delayed feedback methods, in the deterministic inertia ratchet system [20].

On the other hand, starting with the work of Ott, Grebogi, and Yorke [21], various methods for controlling chaotic dynamics have been developed [22]. Particularly, Pyragas proposed a simple and efficient method, which utilizes a control signal with a difference between the present state of the system and the previous state delayed by the period of an unstable periodic orbit (UPO) [23]. This method, which is called the Pyragas method or delayed feedback control, is noninvasive in the sense that the control signal vanishes when the targeted UPO embedded in a chaotic attractor is stabilized. Some limitations on the Pyragas method have been reported [24] and the modifications of the Pyragas method have been proposed to improve its efficiency [25,26]. In particular, Socolar *et al.* presented a method utilizing information from many previous states of the system, and this method is called the *extended time-delay autosynchronization* or the *extended delay feedback* (EDF) [25]. The stability and analytical properties of a delayed feedback system have been also investigated [27].

In this paper, we aim to control transport properties of the deterministic inertia ratchet system. For this purpose, we have controlled a chaotic current of the system to a regular current by stabilizing an unstable periodic orbit which has a desired mean velocity, via the EDF method. Also, we have shown that the EDF method can be utilized for separation of particles in the deterministic inertia ratchet system as a particle's initial condition varies. The rest of the paper is organized as follows. In Sec. II, we have shown transport properties of the unperturbed deterministic inertia ratchet system. In Sec. III, the system controlled via the EDF method has been presented and the linear stability analysis of a periodic orbit in the presence of the EDF has been considered. The limitation on the stability of a periodic orbit has been discussed by the result of numerical analysis. In Sec. IV, via the EDF method, we have shown achievements of the desired transport properties of the system and a separation of particles has also been presented as varying the particle's initial condition. Conclusions are given in Sec. V.

*dawnmail@sogang.ac.kr
†yjpark@sogang.ac.kr
‡chmkim@sogang.ac.kr

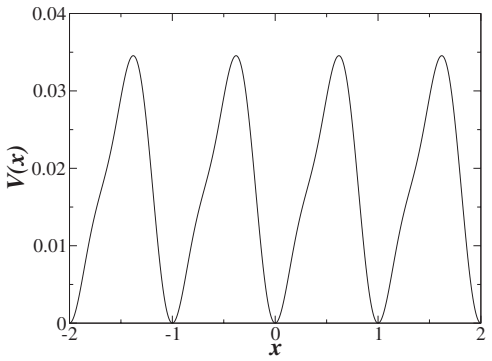

FIG. 1. Asymmetric periodic potential, i.e., the ratchet potential $V(x)=C-\{\sin[2\pi(x-d)]+\frac{1}{4}\sin[4\pi(x-d)]\}/4\pi^2\delta$ with $d=-0.19$, $\delta=\sin(2\pi|d|)+\sin(4\pi|d|)$, and $C=-[\sin(2\pi d)+0.25\sin(4\pi d)]/4\pi^2\delta$.

II. DETERMINISTIC RATCHET SYSTEM

The deterministic inertia ratchet system is written as the following dimensionless equation:

$$\ddot{x}+b\dot{x}+V'(x)=a\cos(\omega_0 t). \tag{1}$$

Here, $V'(x)$ denotes the derivative with respect to x and b is the friction coefficient. ω_0 and a are the frequency and amplitude of the driving force, respectively. Figure 1 shows an asymmetric periodic potential, i.e., the ratchet potential $V(x)$ described by

$$V(x)=C-\left(\sin[2\pi(x-d)]+\frac{1}{4}\sin[4\pi(x-d)]\right)/4\pi^2\delta, \tag{2}$$

where d, δ, and C are introduced so that the ratchet potential has a minimum at $x=0$ with $V(0)=0$.

This system exhibits both regular and chaotic behaviors, depending on parameters (a,b,ω_0) [28–30]. In this paper, we vary only the parameter a, and set $b=0.1$ and $\omega_0=0.67$. General transport properties of the deterministic inertia ratchet system are shown in Fig. 2. In Fig. 2(a), we plot a bifurcation diagram of the stroboscopic recording of a particle's velocity at $t=kT$, where k is a positive integer and T is the period of the driving force. The mean velocity of the system as a function of the parameter a is depicted in Fig. 2(b). As shown in Fig. 2(b), multiple current reversals occur as the amplitude of the driving force is varied. It has also been observed that the current reversal is related to a bifurcation from the chaotic to regular regime [28] and that the type-I intermittency exists in this bifurcation [30] (see also recent papers in Ref. [31]).

When the system exhibits a regular behavior, the time required for a particle to move from one well of the potential to another is commensurable with the period of the driving force. Hence the mean velocity of a regular current shows a locking phenomenon given as follows:

$$\langle v\rangle=\frac{n}{m}\frac{L}{T}=\frac{n}{m}\frac{\omega_0}{2\pi}L=\frac{n}{m}v_l, \tag{3}$$

where L is the spatial period of the ratchet potential ($L=1$, as shown in Fig. 1, then $v_l=\frac{\omega_0}{2\pi}$), T is the time period of the driving force, and $\frac{n}{m}$ is an irreducible fraction $(n,m\in Z)$ [29]. v_l is the fundamental locking velocity corresponding to a particle's current which advances one well of the ratchet potential in a positive direction with the period of the driving force. As shown in Fig. 2, the system exhibits regular behaviors in some parameter ranges; a period-1 orbit with $\langle v\rangle=0$ $(a=0.06)$, a period-2 orbit with $\langle v\rangle=\frac{1}{2}v_l$ $(a=0.074)$, a period-4 orbit with $\langle v\rangle=-\frac{1}{4}v_l$ $(a=0.081)$, and a period-2 orbit with $\langle v\rangle=-\frac{1}{2}v_l$ $(a=0.092)$. When the system shows a chaotic behavior, the mean velocity of the chaotic current is almost zero averaged.

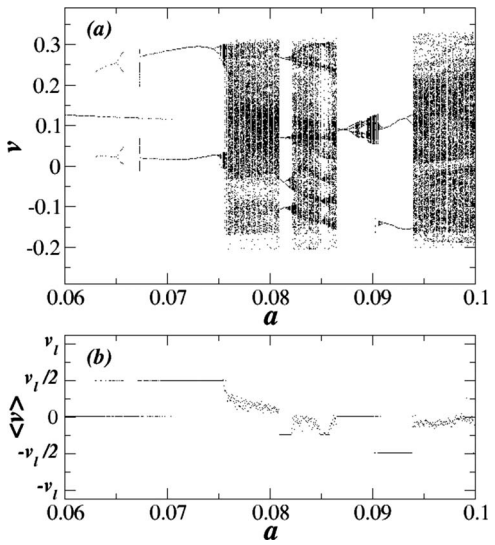

FIG. 2. Bifurcation diagrams as a function of a at $b=0.1$ and $\omega_0=0.67$. In the region from $a=0.063$ to 0.071, coexisting attractors are found; (a) the stroboscopic recording of particle velocity and (b) the mean velocity of current.

It is worthy of note that there are various UPOs embedded in a chaotic attractor of the unperturbed system and that their mean velocities agree with Eq. (3). By stabilizing an UPO that has a desired mean velocity [i.e., written by specific n and m in Eq. (3)], we can achieve a desired regular transport of the deterministic inertia ratchet system instead of the zero averaged chaotic current. In this system, the periodic orbit is defined by $[\tilde{x}(t),v(t)]=[\tilde{x}(t+\tau),v(t+\tau)]$, where $\tilde{x}(t)=x(t)(\mathrm{mod}\ 1)$ and τ is the time period of the orbit. We are interested in stabilizing some targeted UPOs among various UPOs that agree with Eq. (3). In Fig. 3, we have shown several UPOs, which are desired to be stabilized, located by the Newton method. For period-n orbits, we consider two UPOs that have the same period $\tau=nT=2n\pi/\omega_0$ with different mean velocities, where $n=1,2,3,4$: one is a positive current with the mean velocity $\langle v\rangle=\frac{1}{n}v_l$, while the other is a negative current with the mean velocity $\langle v\rangle=-\frac{1}{n}v_l$. Note that the positive and the negative currents are spatially desymmetrized because of asymmetric property of the system. Particularly, period-1 orbits include an oscillating orbit confined in one well of the potential with the mean velocity $\langle v\rangle=0$. By selecting a specific UPO and stabilizing it via the EDF method, we can easily control transport properties of the deterministic inertia ratchet system.

It seems appropriate to comment on the transport phenomenon in the ratchet and nonratchet systems. The nonzero

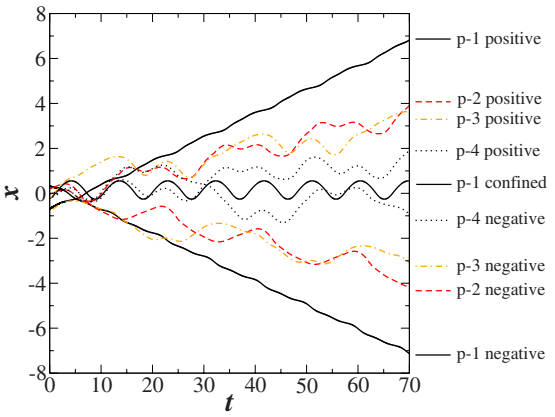

FIG. 3. (Color online) Unstable periodic orbits. Period-1 (solid black line), period-2 (dashed red line), period-3 (dashed-dotted orange line), and period-4 orbits (dotted black line) obtained from the unperturbed system at $a=0.083$.

current of a single particle is less of an interesting phenomenon than the nonzero ensemble averaged current in the ratchet system because the nonzero current of a single particle can also be observed in the nonratchet system, e.g., the asymmetric potential in Eq. (2) is replaced by a symmetric one. Whenever the nonzero current of a single particle that possesses mean velocity (time averaged velocity) v exists, another nonzero current, i.e., symmetry-related pair possessing $-v$, exists as well in the nonratchet system. The symmetric property of the system involves that basins of attraction of two symmetry-related pairs are equivalent and the ensemble averaged velocity results in zero. However, in the ratchet system, broken symmetries cause a desymmetrization of basins of attraction as well as a desymmetrization between spatial profiles of two currents with mean velocities v and $-v$. It induces that the ratchet system has a nonzero ensemble averaged velocity [4].

III. LINEAR STABILITY ANALYSIS OF PERIODIC ORBITS

The deterministic inertia ratchet system controlled by the EDF method is described as

$$\ddot{x} + b\dot{x} + V'(x) = a\cos(\omega_0 t) + F, \tag{4}$$

where F is a control signal, i.e., the delayed feedback described by the particle's present velocity and the previous velocities delayed by multiples of the period of UPO. F is denoted by

$$F = K((1-R)\sum_{m=1}^{\infty} R^{m-1}\dot{x}(t-m\tau) - \dot{x}(t)), \tag{5}$$

where K is a strength of feedback, τ is a delay time, which coincides with the period of the targeted UPO, and R ($0 \le R < 1$) is a parameter that adjusts the distribution of each term's magnitude in the control signal. When $R=0$, the EDF method is the same as the Pyragas method [23], i.e., $F = K[\dot{x}(t-\tau) - \dot{x}(t)]$.

Now, let us consider the linear stability analysis of a periodic orbit in the presence of the EDF. Let the small deviation from the periodic orbit $\boldsymbol{\xi}_0(t)$ be $\delta\boldsymbol{\xi}(t) = \boldsymbol{\xi}(t) - \boldsymbol{\xi}_0(t)$. According to the Floquet theory [32], $\delta\boldsymbol{\xi}(t)$ can be described as

$$\delta\boldsymbol{\xi}(t) = \sum_{k=1}^{N} C^{(k)} e^{(\lambda_k + i\omega_k)t}\boldsymbol{u}_k(t), \tag{6}$$

where $\lambda_k + i\omega_k$ is the Floquet exponent and $\boldsymbol{u}_k(t) = \boldsymbol{u}_k(t+\tau)$ is an eigenvector. $C^{(k)}$ is a constant and N is the dimension of the Poincaré surface. For one such mode, one can obtain the following deviation relation (dropping the index k). After the period τ of the periodic orbit has passed, the deviation is described as

$$\begin{aligned}\delta\boldsymbol{\xi}(t+\tau) &= \exp[(\lambda + i\omega)(t+\tau)]\boldsymbol{u}(t+\tau) \\ &= \exp[(\lambda + i\omega)\tau]\delta\boldsymbol{\xi}(t) \equiv (\Lambda + i\Omega)\delta\boldsymbol{\xi}(t),\end{aligned} \tag{7}$$

where $\Lambda + i\Omega$ is the Floquet multiplier. When the delay terms are included, the phase space of the system becomes infinite dimensional and the system has an infinite number of Floquet multipliers. If the largest Floquet multiplier satisfies $|\Lambda_1 + i\Omega_1| < 1$, i.e., the leading Floquet exponent λ_1 ($\lambda_1 = \ln|\Lambda_1 + i\Omega_1|/\tau$) is less than zero, thereby the targeted UPO is stabilized.

The time evolution of $\delta\boldsymbol{\xi}(t)$ is given by

$$\begin{aligned}\delta\dot{\boldsymbol{\xi}} = &\begin{pmatrix} 0 & 1 \\ -V''(x) & -b \end{pmatrix}\delta\boldsymbol{\xi}(t) + \begin{pmatrix} 0 & 0 \\ 0 & 1 \end{pmatrix}K((1-R)\sum_{m=1}^{\infty} R^{m-1} \\ &\times \delta\boldsymbol{\xi}(t-m\tau) - \delta\boldsymbol{\xi}(t)),\end{aligned} \tag{8}$$

where the matrix in the first term in Eq. (8) is the Jacobian of the unperturbed system and the second term comes from the presence of the EDF. The delayed terms in Eq. (8) can be eliminated and consequently the time evolution of the small deviation from the periodic orbit could be governed by

$$\delta\dot{\boldsymbol{\xi}} = \begin{pmatrix} 0 & 1 \\ -V''(x) & -b - K\dfrac{1 - \frac{1}{\Lambda + i\Omega}}{1 - \frac{R}{\Lambda + i\Omega}} \end{pmatrix}\delta\boldsymbol{\xi}(t) = A\,\delta\boldsymbol{\xi}(t). \tag{9}$$

For an elimination of the delay terms, we use the relation

$$\delta\boldsymbol{\xi}(t - n\tau) = (\Lambda + i\Omega)^{-n}\delta\boldsymbol{\xi}(t) \quad (n = 1,2,3,\ldots). \tag{10}$$

Equation (9) requires information of the targeted UPO. Hence the Floquet multiplier is related to the eigenvalue problem of the monodromy matrix Φ_τ, which satisfies

$$\dot{\Phi}_t = A\Phi_t, \quad \Phi_0 = I. \tag{11}$$

The eigenvalue of Φ_τ defines the Floquet multiplier as follows:

$$\det[\Phi_\tau - (\Lambda + i\Omega)I] = 0; \tag{12}$$

but, since the solutions of Eq. (12) cannot be obtained analytically, we calculate Floquet multipliers by applying the Newton method to Eq. (12). Several branches of Floquet multiplier are concerned in a determination of the largest Floquet multiplier and the corresponding leading Floquet exponent, λ_1. For all periodic orbits that the results of λ_1 are shown in Figs. 5–8, the process for determination of λ_1 can

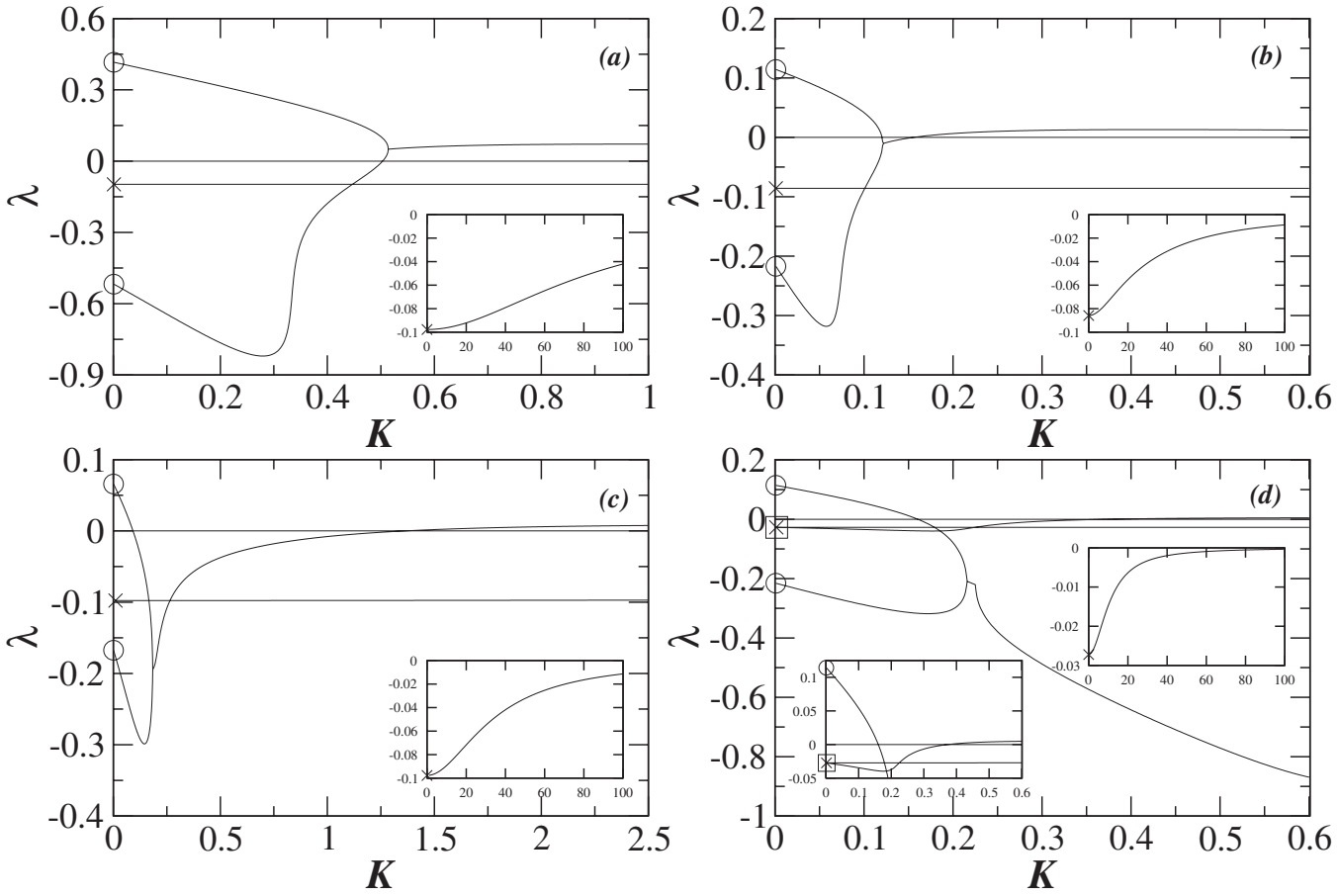

FIG. 4. Several branches of Floquet exponent; (a)–(d) exhibit the process for determining λ_1 of the period-1 positive ($R=0.4$), the period-2 negative ($R=0.2$), the period-1 confined ($R=0.4$), and the period-2 negative ($R=0.6$) currents, respectively.

be categorized into four different types and it is shown in Fig. 4.

All periodic orbits in Fig. 3, except for the period-3 positive orbit, have common properties. When $K=0$, two Floquet multipliers of the unperturbed periodic orbit are real and negative so that the corresponding Floquet exponents satisfy $\omega=\pi/\tau$. It means that all UPOs flip their neighborhood within the period τ in the unperturbed system. However, the unperturbed period-3 positive orbit has two real positive Floquet multipliers so that it cannot be stabilized by the EDF method. It has been known that the delayed feedback method, including the EDF method, can stabilize only a certain class of periodic orbits with a finite torsion [24]. In Fig. 4(a), we plot several branches of Floquet exponent, which participate in the determination of λ_1 for the period-1 positive current ($R=0.4$). Two Floquet exponents of the unperturbed orbit are denoted by open circles. As K increases, two Floquet exponents approach each other in remaining real negative Floquet multipliers. Then, two branches collide at $K\simeq 0.51$ and the pair of Floquet exponents, i.e., complex conjugates Floquet multipliers, generate. It is precisely at this point that λ_1 has a local minimum value. With the further increase of K, λ of the generated branch increases for some intervals of K. For $K\to\infty$, the pair of generated Floquet multipliers move toward $(\Lambda,\Omega)=(1,0)$ so that λ approaches the zero line.

There is another branch of Floquet exponent that does not arise from the unperturbed periodic orbit. It depends on the presence of EDF. When the loop of EDF is turned on, i.e., for nonzero infinitesimal K, the pair of complex roots for Eq. (12) emerge at (Λ,Ω) and $(\Lambda,-\Omega)$, which are very close to $(R,0)$ (Λ is infinitesimally larger than R and Ω is slightly deviated from 0). The corresponding Floquet exponent is depicted by the cross point in Fig. 4(a) and is located infinitesimally larger than $\lambda=\ln(R)/\tau=\ln(0.4)/(2\pi/\omega_0)\simeq -0.0977$. Though the branch originating from the EDF looks like a constant line in Fig. 4(a), it increases very slowly. As K increases, the pair of complex roots arising from the EDF move toward $(\Lambda,\Omega)=(1,0)$ so that the corresponding Floquet exponent approaches the zero line very slowly [see inset of Fig. 4(a)]. Consequently, λ_1 for period-1 positive current ($R=0.4$) is determined by a combination of two branches; one is originating from the initially unstable Floquet exponent and the other is generated by the collision of two branches arising from the unperturbed periodic orbit. The branch originating from the EDF does not affect the determination of λ_1 in Fig. 4(a). The above process makes the minimum of λ_1 larger than zero so that the period-1 positive current cannot be stabilized at $R=0.4$ [see the result of λ_1 in Fig. 5(a) for $R=0.4$].

The process for determining λ_1 of the period-2 negative current ($R=0.2$) is depicted in Fig. 4(b) and has an analogy

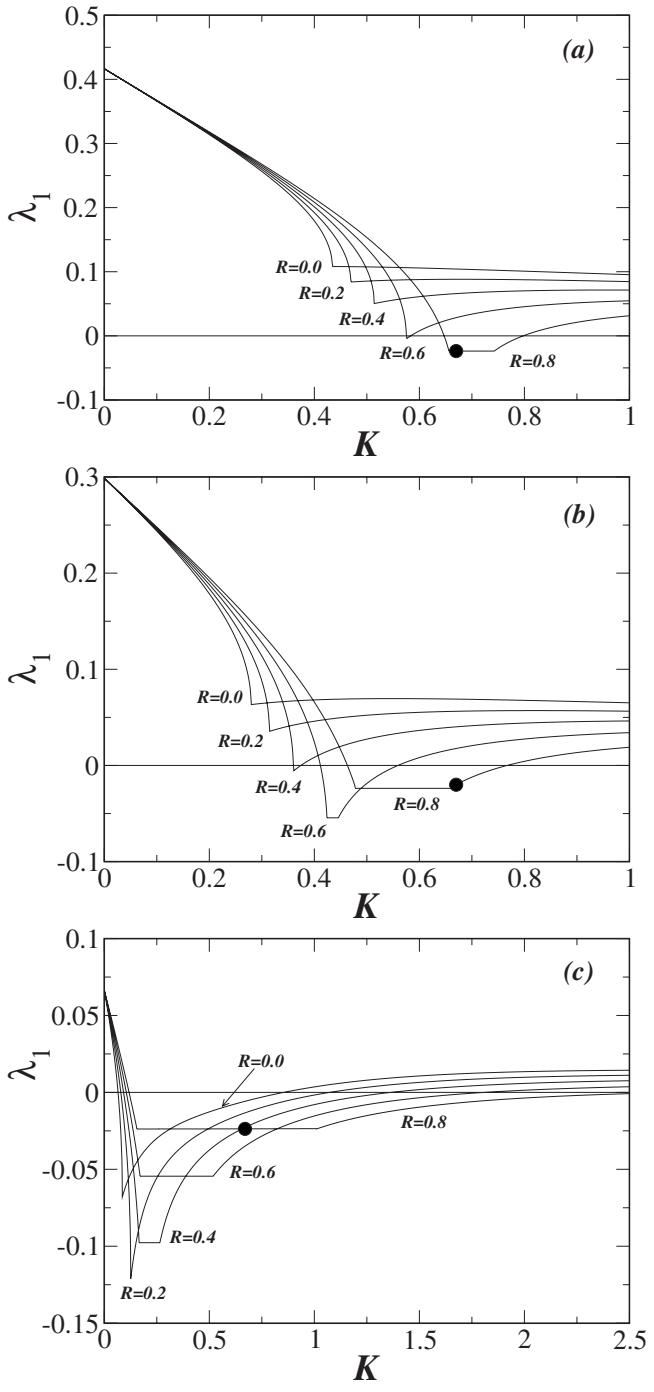

FIG. 5. The leading Floquet exponents of period-1 orbits; (a)–(c) exhibit the leading Floquet exponents for the positive, the negative, and the confined currents as a function of K for the given R, respectively.

with that of Fig. 4(a). The only difference is that two branches arising from the unperturbed periodic orbit collide at $\lambda<0$. For the further increase of K, λ of the generated branch increases and crosses the zero line so that the period-2 negative current has a finite stabilized interval of $K\in[K_{\min},K_{\max}]$. $K_{\min}$ is determined by the crossing of the initially unstable branch into the zero line, and the crossing of the generated branch into the zero line decides $K_{\max}$ [see the result of λ_1 in Fig. 6(b) for $R=0.2$].

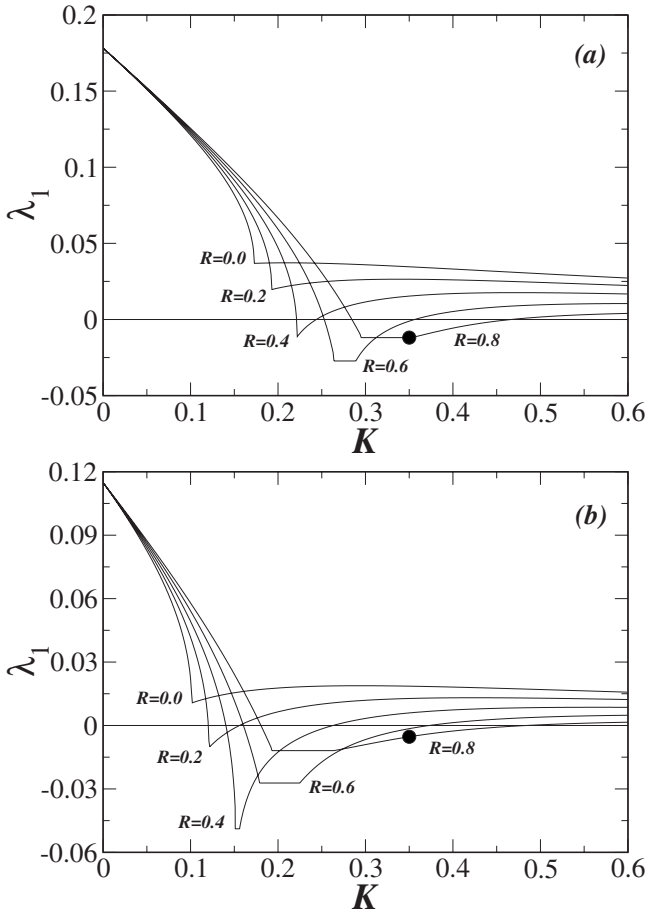

FIG. 6. The leading Floquet exponents of period-2 orbits; (a) and (b) exhibit the leading Floquet exponents for the positive and the negative currents as a function of K for the given R, respectively.

In Fig. 4(c), the branch originating from the EDF plays a role in determining λ_1 for the period-1 confined current ($R=0.4$). The branch arising from the initially unstable Floquet exponent crosses the branch from the EDF at $K\simeq 0.17$. Two branches evolve independently from each other and then the initially unstable branch collides with the initially stable branch. For the further increase of K, the generated branch crosses the EDF branch again. So, the shape of λ_1 makes a valley with a flat bottom and the first crossing between the initially unstable branch and the branch arising from the EDF makes the minimum of λ_1, which is infinitesimally larger than $\lambda=\ln(0.4)/(2\pi/\omega_0)\simeq -0.0977$ at $K\simeq 0.17$ [see the result of λ_1 in Fig. 5(c) for $R=0.4$].

In Fig. 4(d), a new branch of Floquet exponent arising from the EDF is concerned in the determination of λ_1 for the period-2 negative current ($R=0.6$). With an analogy of the cross point, for nonzero infinitesimal K, the pair of complex roots for Eq. (12) emerge at (Λ,Ω) and $(\Lambda,-\Omega)$, which are very close to $(R,0)$ (Λ is infinitesimally "smaller" than R and Ω is slightly deviated from 0). The corresponding Floquet exponent is depicted by the open square in Fig. 4(d) and is located infinitesimally "smaller" than $\lambda=\ln(0.6)/(4\pi/\omega_0)\simeq -0.0272$. The new branch arising from the open square evolves independently from other branches, which is similar

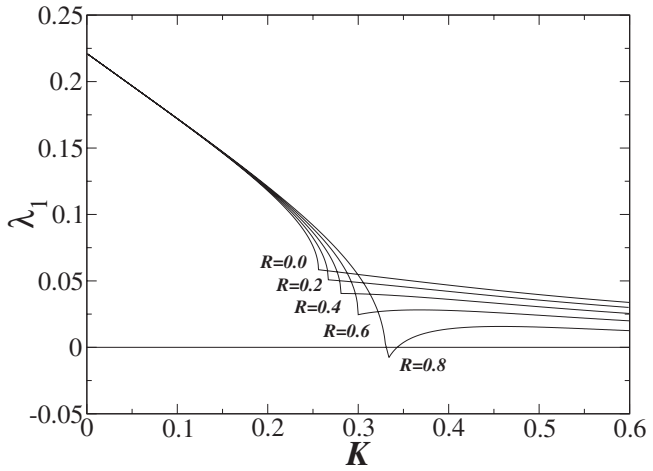

FIG. 7. The leading Floquet exponent of the period-3 positive orbit as a function of K for the given R.

to the evolution of the branch arising from the cross point. For small ranges of K, λ of the new branch decreases. For the further increase of K, the new branch from the open square crosses the branch from the cross point and the zero line [see the lower inset of Fig. 4(d)]. The upper boundary of the stabilized interval of K, i.e., $K_{\max}$, is determined by the crossing of the branch from the open square into the zero line. It is quite different for the case of Figs. 4(b) and 4(c). λ of the generated branch decreases continually and the generated branch does not play a dominant role for determining λ_1 in this case. With an analogy of Fig. 4(c), the shape of λ_1 makes a valley with a flat bottom and the crossing of the initially unstable branch into the branch arising from the cross point makes the minimum of λ_1, which is infinitesimally larger than $\lambda=\ln(0.6)/(4\pi/\omega_0)\simeq-0.0272$ [see the result of λ_1 in Fig. 6(b) for $R=0.6$].

The results of λ_1 are shown in Figs. 5–8 for period-1 ($\tau=T=2\pi/\omega_0$), period-2 ($\tau=2T$), period-3 ($\tau=3T$), and period-4 orbits ($\tau=4T$), respectively. Each figure shows λ_1 as a function of the strength of feedback K for different values of the control parameter R. The results tell us the stabilized region of control parameters (K,R,τ), in which the targeted UPO is stabilized ($\lambda_1<0$). The process for determining λ_1 of periodic orbits in Figs. 5–8 is categorized as follows; periodic orbits which cannot be stabilized by the EDF method ($\lambda_1>0$) are equivalent to Fig. 4(a), and periodic orbits, which have a finite stabilized region of K depicted by a narrow valley, are equivalent to Fig. 4(b). Periodic orbits, which have a finite stabilized region depicted by a valley with a flat bottom, are twofold. The period-1 positive ($R=0.8$), the period-1 negative ($R=0.6,0.8$), and the period-1 confined currents ($R=0.4,0.6,0.8$) are equivalent to Fig. 4(c). Figure 4(d) shows the process of the period-2 positive ($R=0.6$, 0.8), the period-2 negative ($R=0.6,0.8$), and the period-4 negative currents ($R=0.4,0.6,0.8$).

The results in Figs. 5–8 verify well-known properties of the EDF method [27]; with the larger degree of instability in the unperturbed system, the UPO can be stabilized with a larger R and the stabilized region of K for the given R increases as R increases. The period-4 positive current cannot be stabilized at $R\leq0.8$ because it has a greater degree of

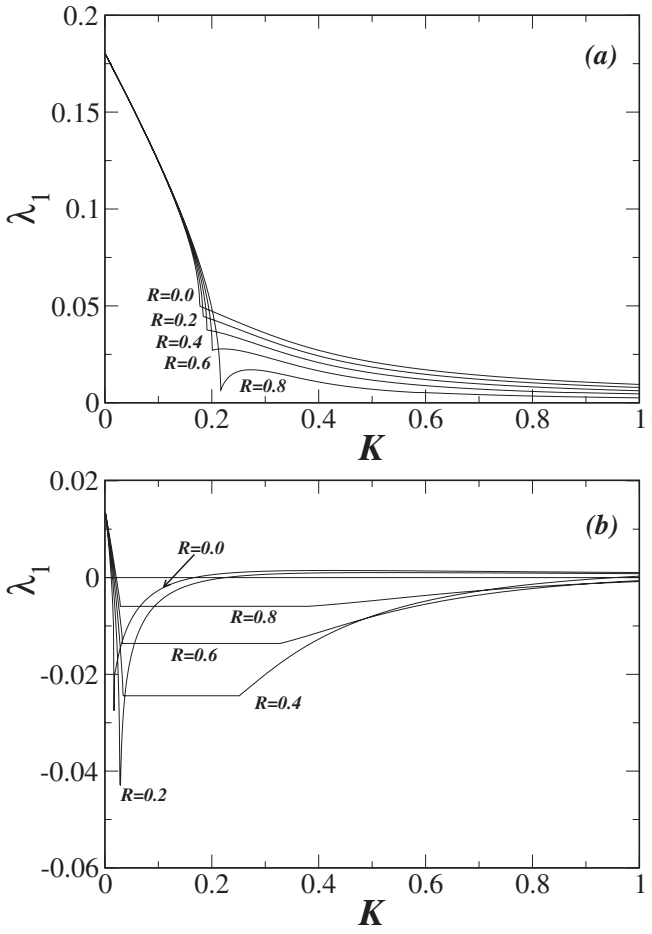

FIG. 8. The leading Floquet exponents of period-4 orbits; (a) and (b) exhibit the leading Floquet exponents for the positive and the negative currents as a function of K for the given R, respectively.

instability ($\Lambda_1\simeq-862,\Omega_1=0$) in the unperturbed system. If R is not very large so that the branch originating from the EDF (arising from the cross point in Fig. 4) does not take a leading branch, then the minimum of λ_1 is deeper as R increases. The numerical analysis in Fig. 4 presents explicitly an interesting property of the EDF method, i.e., the limitation on the minimum of λ_1 for given control parameters R and τ. For any nonzero R, the branch arising from the cross point exists so that λ_1 cannot be smaller than $\lambda=\ln(R)/\tau$.

IV. CONTROL OF TRANSPORT PROPERTIES

With the results of linear stability analysis of periodic orbits, we can obtain a desired transport property of the system (i.e., a regular current with a desired mean velocity) by choosing the control parameters (K,R,τ) where the corresponding UPO is stabilized. For simple and efficient application of the EDF method, it is hoped that each UPO has its own stabilized region of control parameters, in which the other UPOs still remain in an unstable state. Some of the UPOs have their own stabilized regions of control parameters. These orbits are the period-1 confined, the period-2 negative, the period-3 positive, and the period-4 negative

currents. For the cases of the period-1 positive, the period-1 negative, and the period-2 positive currents, the stabilization of each periodic orbit is rather complex because they do not have their own stabilized regions of control parameters. The stabilized region of the period-1 positive and the negative currents always overlaps with that of the period-1 confined current, and the stabilized region of the period-2 positive current overlaps with that of the period-2 negative current.

Now, we are interested in the multistable phenomenon that more than one UPO is stabilized at the same control parameters (K,R,τ). At control parameters, $K=0.67$, $R=0.8$, and $\tau=T=2\pi/\omega_0$, all of period-1 orbits are stabilized. In Fig. 5, each of the leading Floquet exponents of the period-1 orbits at theses parameters is marked by a black circle and all of them are less than zero. Also, all of the period-2 orbits are stabilized at $K=0.35$, $R=0.8$, and $\tau=2T=4\pi/\omega_0$. Each of the leading Floquet exponents of the period-2 orbits at these parameters is marked by a black circle in Fig. 6. In the unperturbed system $(K=0)$, all of the initial conditions evolve into a chaotic current in the same manner. However, the system controlled by the EDF method shows different currents for different initial conditions (x_0,v_0) at control parameters where the multistable phenomenon is observed.

Before considering the numerical integration for obtaining dynamics of the system controlled by the EDF method, we rewrite the control signal $F(t)$ given in Eq. (5) into a more convenient form:

$$F(t) = K[(1-R)S(t-\tau) - \dot{x}(t)],$$

$$S(t) = \dot{x}(t) + RS(t-\tau), \tag{13}$$

where $S(t)=\Sigma_{m=0}^{\infty}R^m\dot{x}(t-m\tau)$ for an equivalent equation with Eq. (5) (see Ref. [33]). In the following numerical integrations, we set $S(t')=0$ for t' in the interval $[-\tau,0]$ and initialize $S(t')=\dot{x}(t')/(1-R)$ for t' in the interval $[0,\tau]$. Then, the system is not perturbed $(F=0)$ for t in the interval $[0,\tau]$ and perturbed by the control signal from $t=\tau$. In Fig. 9, we have plotted three stabilized period-1 orbits that evolved from different initial conditions and the dynamics of the control signal F at the same control parameters, $K=0.67$, $R=0.8$, and $\tau=T=2\pi/\omega_0$. For each initial condition, we have integrated Eqs. (4) and (13). In Fig. 10, we have shown two stabilized period-2 orbits that evolved from different initial conditions and the dynamics of the control signal F at $K=0.35$, $R=0.8$, and $\tau=2T=4\pi/\omega_0$. The multistable phenomenon shows that the EDF method can be utilized for separation of particles in the deterministic inertia ratchet system. Via the EDF method, we can separate particles in the deterministic inertia ratchet system as their initial conditions vary. Note that the method for extracting information of a single particle trajectory from the sea of trajectories with an ensemble of particles and the feedback scheme, which assure a particle is only affected by its own previous states, are not considered in the level of real experimental situations. In our work, the application for separation of particles is conceptually discussed.

In Fig. 11, we have investigated the basins of period-1 and period-2 orbits. We have integrated Eqs. (4) and (13) with the initial condition (x_0,v_0) at $K=0.67$, $R=0.8$, $\tau=T=2\pi/\omega_0$ [in Fig. 11(a)] and at $K=0.35$, $R=0.8$, $\tau=2T=4\pi/\omega_0$ [in Fig. 11(b)]. x_0 and v_0 are uniformly distributed in $x_0\in(-0.38,0.62)$, one well of the potential, and $v_0\in(-0.3,0.3)$, the ranges of velocities in the unperturbed system. As shown in Fig. 11(a), the basins of the period-1 positive, the negative, and the confined currents are marked by □ (orange), △ (red), and · (black), respectively. The basins of the period-2 positive and the negative currents are marked by · (black) and △ (red), respectively, in Fig. 11(b).

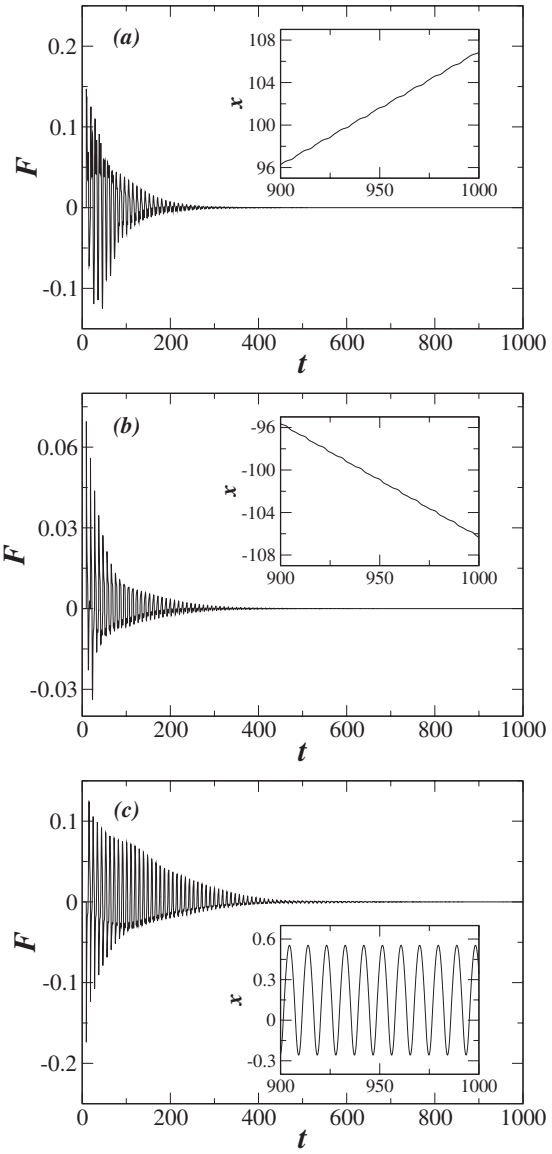

FIG. 9. Stabilized period-1 orbits (insets) and the dynamics of the control signal F at $K=0.67$, $R=0.8$, and $\tau=T=2\pi/\omega_0$; (a) the positive current from the initial condition $(x_0,v_0)=(-0.35,0.2)$, (b) the negative current from (0.2, 0.0), and (c) the confined current from (0.0, 0.0).

In contrast with the separation of particles, a unified phenomenon of the ratchet system can be obtained by altering the control force F of the EDF. We have replaced the term representing previous velocities of a single particle in Eq. (5) by ensemble averaged previous velocities as follows:

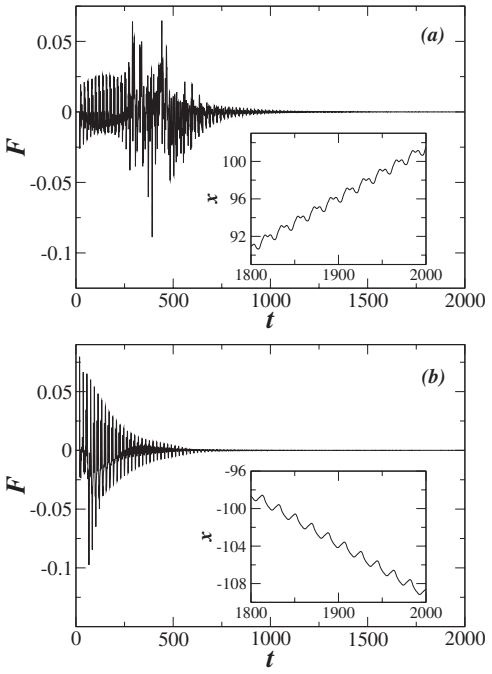

FIG. 10. Stabilized period-2 orbits (insets) and the dynamics of the control signal F at $K=0.35$, $R=0.8$, and $\tau=2T=4\pi/\omega_0$; (a) the positive current from the initial condition $(x_0,v_0)=(0.0,0.0)$, and (b) the negative current from (0.0, 0.1).

$$F = K((1-R)\sum_{m=1}^{\infty} R^{m-1}\tilde{x}(t-m\tau) - \dot{x}(t)), \qquad (14)$$

where $\tilde{x}(t-m\tau)=\frac{1}{N}\Sigma_{i=1}^{N}\dot{x}_i(t-m\tau)$ and the initial condition of the ith particle, (x_{0_i},v_{0_i}) is uniformly distributed in $x_{0_i} \in (-0.38,0.62)$ and $v_{0_i} \in (-0.3,0.3)$. We have calculated same integrations in Fig. 11 by applying the control force given in Eq. (14). Then, at the same control parameters with Fig. 11(a), all of the initial conditions evolve into the period-1 confined current so that the basin of attraction of the period-1 confined current fills the whole phase space shown in Fig. 11(a). Note that the basin of the period-1 confined current is the largest one in Fig. 11(a). Equivalently, all of the initial conditions evolve into the period-2 positive current at the same control parameters with Fig. 11(b). In the ratchet system feedbacked by ensemble averaged velocities, a property of the unified current is determined by a current, which has the largest basin of attraction in the system feedbacked by its own previous states.

V. CONCLUSIONS

We have studied the control of transport properties in the deterministic inertia ratchet system via the extended delay feedback method. We have controlled a chaotic current of the unperturbed system to a regular current, which has a desired mean velocity. To obtain the control parameters in which the corresponding unstable periodic orbit is stabilized, we have solved the leading Floquet exponent in the presence of the extended delay feedback. By the numerical analysis, it has been explicitly presented that the limitation on the minimum of the leading Floquet exponent exists for given control parameters of the EDF. With the results of leading Floquet exponents as a function of control parameters, we have obtained a desired regular transport property of the system. Also, we have observed the multistable phenomenon that more than one unstable periodic orbit is stabilized at the same control parameters and we have shown that the extended delay feedback method can be utilized for separation of particles as a particle's initial condition varies. Moreover, we have shown that the unified phenomenon of the ratchet system has been also observed by applying the ensemble averaged feedback.

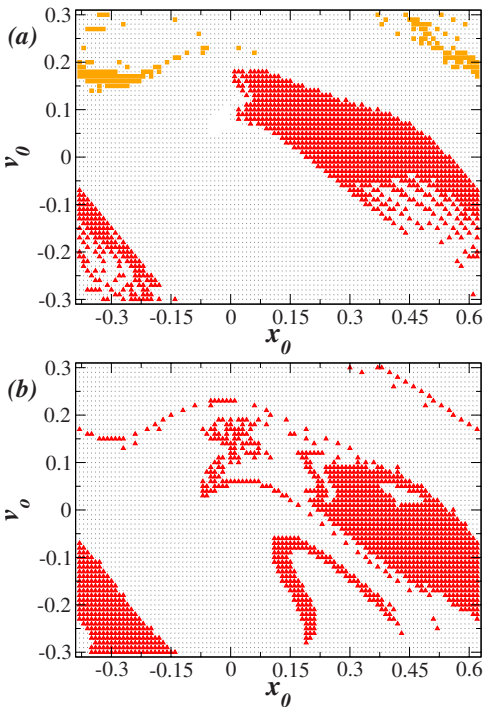

FIG. 11. (Color online) (a) Basins of period-1 orbits; the initial points marked by □ (orange), △ (red), and · (black) are the basins of the positive, the negative, and the confined currents, respectively. (b) Basins of period-2 orbits; the initial points marked by · (black) and △ (red) are the basins of the positive and the negative currents, respectively.

ACKNOWLEDGMENTS

The authors thank Dr. S. Rim for valuable discussions. C.-M.K. is supported by Sogang Research Grant No. 20071114.

[1] P. Reimann, Phys. Rep. **361**, 57 (2002).
[2] R. D. Astumian and P. Hänggi, Phys. Today **55**, 33 (2002); P. Hänggi, F. Marchesoni, and F. Nori, Ann. Phys. **14**, 51 (2005).
[3] R. D. Astumian and M. Bier, Phys. Rev. Lett. **72**, 1766 (1994); Biophys. J. **70**, 637 (1996); M. Porto, M. Urbakh, and J. Klafter, Phys. Rev. Lett. **85**, 491 (2000); J. V. Hernández, E. R. Kay, and D. A. Leigh, Science **306**, 1532 (2004).
[4] S. Flach, O. Yevtushenko, and Y. Zolotaryuk, Phys. Rev. Lett. **84**, 2358 (2000).
[5] P. Jung, J. G. Kissner, and P. Hänggi, Phys. Rev. Lett. **76**, 3436 (1996).
[6] H. Schanz, M.-F. Otto, R. Ketzmerick, and T. Dittrich, Phys. Rev. Lett. **87**, 070601 (2001); S. Denisov, S. Flach, A. A. Ovchinnikov, O. Yevtushenko, and Y. Zolotaryuk, Phys. Rev. E **66**, 041104 (2002); N. A. C. Hutchings, M. R. Isherwood, T. Jonckheere, and T. S. Monteiro, *ibid.* **70**, 036205 (2004); H. Schanz, T. Dittrich, and R. Ketzmerick, *ibid.* **71**, 026228 (2005).
[7] L. Machura, M. Kostur, P. Talkner, J. Łuczka, F. Marchesoni, and P. Hänggi, Phys. Rev. E **70**, 061105 (2004); H. Chen, Q. Wang, and Z. Zheng, *ibid.* **71**, 031102 (2005); L. Machura, M. Kostur, F. Marchesoni, P. Talkner, P. Hänggi, and J. Łuczka, J. Phys.: Condens. Matter **17**, S3741 (2005); M. Kostur, L. Machura, and P. Hänggi, J. Łuczka, and P. Talkner, Physica A **371**, 20 (2006); D. Speer, R. Eichhorn, and P. Reimann, Phys. Rev. E **76**, 051110 (2007).
[8] I. Zapata, R. Bartussek, F. Sols, and P. Hänggi, Phys. Rev. Lett. **77**, 2292 (1996); C. C. de Souza Silva, J. V. de Vondel, M. Morelle, and V. V. Moshchalkov, Nature (London) **440**, 651 (2006).
[9] P. Reimann, M. Grifoni, and P. Hänggi, Phys. Rev. Lett. **79**, 10 (1997); M. Grifoni, M. S. Ferreira, J. Peguiron, and J. B. Majer, *ibid.* **89**, 146801 (2002).
[10] K. H. Lee, Appl. Phys. Lett. **83**, 117 (2003); D. E. Shalóm and H. Pastoriza, Phys. Rev. Lett. **94**, 177001 (2005); M. Beck, E. Goldobin, M. Neuhaus, M. Siegel, R. Kleiner, and D. Koelle, *ibid.* **95**, 090603 (2005); K. H. Lee, J. Korean Phys. Soc. **47**, 288 (2005).
[11] J. Rousselet, L. Salome, A. Ajdari, and J. Prost, Nature (London) **370**, 446 (1994).
[12] M. N. Popescu, C. M. Arizmendi, A. L. Salas-Brito, and F. Family, Phys. Rev. Lett. **85**, 3321 (2000); C. M. Arizmendi, F. Family, and A. L. Salas-Brito, Phys. Rev. E **63**, 061104 (2001); M. N. Popescu, C. M. Arizmendi, A. L. Salas-Brito, and F. Family, Phys. Rev. Lett. **88**, 049903(E) (2002); L. Gao, X. Luo, S. Zhu, and B. Hu, Phys. Rev. E **67**, 062104 (2003).
[13] R. Bartussek, P. Reimann, and P. Hänggi, Phys. Rev. Lett. **76**, 1166 (1996); T. E. Dialynas, K. Lindenberg, and G. P. Tsironis, Phys. Rev. E **56**, 3976 (1997).
[14] M. O. Magnasco, Phys. Rev. Lett. **71**, 1477 (1993); I. Derényi and T. Vicsek, *ibid.* **75**, 374 (1995).
[15] M. Barbi and M. Salerno, Phys. Rev. E **63**, 066212 (2001).
[16] S. Savel'ev, F. Marchesoni, P. Hänggi, and F. Nori, Phys. Rev. E **70**, 066109 (2004).
[17] D. Goldobin, M. Rosenblum, and A. Pikovsky, Phys. Rev. E **67**, 061119 (2003); J.-W. Ryu, W.-H. Kye, S.-Y. Lee, M.-W. Kim, M. Choi, S. Rim, Y.-J. Park, and C.-M. Kim, *ibid.* **70**, 036220 (2004).
[18] F. J. Cao, L. Dinis, and J. M. R. Parrondo, Phys. Rev. Lett. **93**, 040603 (2004); M. Feito and F. J. Cao, Phys. Rev. E **76**, 061113 (2007); D. Wu, S. Zhu, and X. Luo, Phys. Lett. A **372**, 2002 (2008).
[19] M. Kostur, P. Hänggi, P. Talkner, and J. L. Mateos, Phys. Rev. E **72**, 036210 (2005).
[20] W.-S. Son, Y.-J. Park, J.-W. Ryu, D.-U. Hwang, and C.-M. Kim, J. Korean Phys. Soc. **50**, 243 (2007).
[21] E. Ott, C. Grebogi, and J. A. Yorke, Phys. Rev. Lett. **64**, 1196 (1990).
[22] T. Shinbrot, C. Grebogy, E. Ott, and J. A. Yorke, Nature (London) **363**, 411 (1993); *Handbook of Chaos Control*, edited by H. G. Schuster (Wiley-VCH, Weiheim, 1999); S. Boccaletti, C. Grebogi, Y.-C. Lai, H. Mancini, and D. Maza, Phys. Rep. **329**, 103 (2000).
[23] K. Pyragas, Phys. Lett. A **170**, 421 (1992).
[24] T. Ushio, IEEE Trans. Circuits Syst., I: Fundam. Theory Appl. **43**, 815 (1996); W. Just, T. Bernard, M. Ostheimer, E. Reibold, and H. Benner, Phys. Rev. Lett. **78**, 203 (1997); H. Nakajima, Phys. Lett. A **232**, 207 (1997); H. Nakajima and Y. Ueda, Physica D **111**, 143 (1998).
[25] J. E. S. Socolar, D. W. Sukow, and D. J. Gauthier, Phys. Rev. E **50**, 3245 (1994).
[26] A. Kittel, J. Parisi, and K. Pyragas, Phys. Lett. A **198**, 433 (1995); H. G. Schuster and M. P. Stemmler, Phys. Rev. E **56**, 6410 (1997); K. Pyragas, Phys. Rev. Lett. **86**, 2265 (2001).
[27] M. E. Bleich and J. E. S. Socolar, Phys. Lett. A **210**, 87 (1996); W. Just, E. Reibold, H. Benner, K. Kacperski, P. Fronczak, and J. A. Hołyst, *ibid.* **254**, 158 (1999); W. Just, E. Reibold, K. Kacperski, P. Fronczak, J. A. Hołyst, and H. Benner, Phys. Rev. E **61**, 5045 (2000); K. Pyragas, *ibid.* **66**, 026207 (2002); W. Just, H. Benner, and C. von Loewenich, Physica D **199**, 33 (2004).
[28] J. L. Mateos, Phys. Rev. Lett. **84**, 258 (2000).
[29] M. Barbi and M. Salerno, Phys. Rev. E **62**, 1988 (2000).
[30] W.-S. Son, I. Kim, Y.-J. Park, and C.-M. Kim, Phys. Rev. E **68**, 067201 (2003).
[31] A. Kenfack, S. M. Sweetnam, and A. K. Pattanayak, Phys. Rev. E **75**, 056215 (2007); F. R. Alatriste and J. L. Mateos, Physica A **384**, 223 (2007).
[32] J. K. Hale and S. M. Verduyn Lunle, *Introduction to Functional Differential Equations* (Springer, New York, 1993).
[33] K. Pyragas, Phys. Lett. A **206**, 323 (1995).